JOURNAL OF SOLID STATE CHEMISTRY 42, 22–27 (1982)

The Phase Relations in the Yb_2O_3–Fe_2O_3–*MO* Systems in Air at High Temperatures (*M*: Co, Ni, Cu, and Zn)

NOBORU KIMIZUKA* AND EIJI TAKAYAMA

National Institute for Research in Inorganic Materials, 1-1, Namiki, Sakuramura, Niiharigun, Ibaraki-ken 305, Japan

Received August 24, 1981; in revised form November 13, 1981

The phase relations in the Yb_2O_3–Fe_2O_3–CoO system at 1350 and 1300°C, the Yb_2O_3–Fe_2O_3–NiO system at 1300 and 1200°C, the Yb_2O_3–Fe_2O_3–CuO system at 1000°C, and the Yb_2O_3–Fe_2O_3–ZnO system at 1300°C were determined in air by means of a classical quenching method. New layered-type compounds, $YbFeCoO_4$ (a = 3.4295(5) Å, c = 25.198(3) Å), $YbFeCuO_4$ (a = 3.4808(2) Å, c = 24.100(2) Å), and $YbFeZnO_4$ (a = 3.4251(2) Å, c = 25.282(2) Å), which are isomorphous with $YbFe_2O_4$ (space group: $R\bar{3}m$; a = 3.455(1) Å, c = 25.109(2) Å), and a new compound, $Yb_2Cu_2O_5$, were obtained. In the Yb_2O_3–Fe_2O_3–NiO system, there are no quaternary compounds.

Introduction

In the phase diagrams of the Ln_2O_3–FeO–Fe_2O_3 systems at 1200°C (*Ln:* Y, Ho, Er, Tm, Yb, and Lu), there are $LnFe_2O_4$ compounds with layered structures and their standard free energies of formation were reported by Kimizuka and Katsura and co-workers (*1–3*). As an example, the phase diagram of the Yb_2O_3–FeO–Fe_2O_3 system at 1200°C is illustrated with equilibrium oxygen partial pressures in Fig. 1 (*2*). The crystal structure analyses of $YbFe_2O_4$ and $Yb_2Fe_3O_7$ were performed by Kato *et al.* (*4–5*). Recently Kimizuka and Takayama prepared a series of new compounds $LnA^{2+}B^{3+}O_4$ (*A:* Mg, Mn, Co, Cu, and Zn; *B:* Fe, Ga, and Al) which are isomorphous with $YbFe_2O_4$, and reported the lattice constants and the synthetic conditions of about 50 compounds (*6–7*).

In the present article, we report the phase diagrams of the Yb_2O_3–Fe_2O_3–CoO system at 1350 and 1300°C, the Yb_2O_3–Fe_2O_3–NiO system at 1300 and 1200°C, the Yb_2O_3–Fe_2O_3–CuO system at 1000°C, and the Yb_2O_3–Fe_2O_3–ZnO system at 1300°C. Each phase diagram was determined in air by means of a classical quenching method.

Experimental

Starting materials. Yb_2O_3(99.9%), Fe_2O_3 (99.9%), and reagent-grade Co_2O_3, ZnO, NiO, and CuO were used. Prior to use, Yb_2O_3, Fe_2O_3, Co_2O_3, and ZnO were heated in air at 1300°C for several days. CoO was obtained by reduction of Co_2O_3 (*8*). NiO was heated in air at 1200°C for 3 days. CuO was heated at 1000°C in air for 3 days (*9*). Each of the heat-treated samples was identified from the ASTM cards. The pretreated starting materials were thoroughly mixed to the desired ratios in an agate mortar with ethyl alcohol.

Instruments. A Pt crucible was used as

* To whom correspondence should be addressed.

0022-4596/82/040022-06$02.00/0

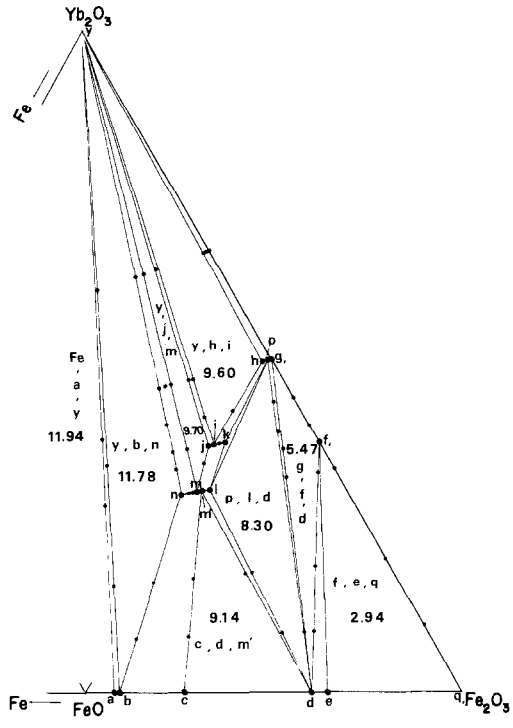

FIG. 1. The phase diagram of the Yb_2O_3–FeO–Fe_2O_3 system at 1200°C. Numbers in the three solid phases indicate the equilibrium oxygen partial pressure in log P_{O_2}(atm). See Ref. (*2*) for detail.

a sample container. Two vertical-type quench furnaces with heating elements of SiC and Rh-alloyed Pt were used. Both furnace temperatures were controlled to within ±1°C. Temperature measurement was made by a Pt–13%RhPt thermocouple calibrated on the gold point. The constant temperature region was about 3 cm long for each furnace. The phase diagrams at 1350 and 1300°C were determined in the SiC furnace and those at 1200 and 1000°C were made in the Pt furnace.

Procedure. About 1000 mg of each sample was placed in a Pt crucible and was heated in the furnace. After heating for 24 hr, the sample was quenched to room temperature and crushed in an agate mortar. The samples were then analyzed by means of powder X-ray diffraction. (Fe$K\alpha$ radiation, a Mn-filtered scintillation counter, and silicon powder as a standard material were used.) This procedure was repeated until the powder X-ray pattern of the sample did not change. It took 7–10 days for the sample to react fully. Sample weights were checked before and after heat treatments.

Results and Discussion

1a. The Yb_2O_3–Fe_2O_3–CoO System at 1350°C in Air

In the Yb_2O_3–Fe_2O_3 system, there were two ternary stable phases, $YbFeO_3$ and $Yb_3Fe_5O_{12}$. The reaction rates between Yb_2O_3 and Fe_2O_3 necessary to form these two compounds were so large that each single phase was obtained within 2 days. Schneider *et al.* (*10*) reported the phase diagram of the Yb_2O_3–Fe_2O_3 system at 1350°C in air. Their results are consistent with the present study. In the Fe_2O_3–CoO system, Fe_2CoO_4 was a stable phase. In the Yb_2O_3–CoO system, there were no ternary phases. In the Yb_2O_3–Fe_2O_3–CoO system, there was a stable quaternary $YbFeCoO_4$. $YbFeCoO_4$ (a = 3.4295(5) Å, c = 25.198(3) Å) is isomorphous with $YbFe_2O_4$ (space group: $R\bar{3}m$; a = 3.455(1) Å, c = 25.109(2) Å) (*6*). No solid solution range in each phase was detected. The phase diagram of the Yb_2O_3–Fe_2O_3–CoO system at 1350°C in air is shown in Fig. 2a.

1b. The Yb_2O_3–Fe_2O_3–CoO System at 1300°C in Air

In the Yb_2O_3–Fe_2O_3 system, the Fe_2O_3–CoO system, and the CoO–Yb_2O_3 system, there were the same phases as in those at 1350°C. In the Yb_2O_3–Fe_2O_3–CoO system, there were no stable quaternary phases. After the first heating of the mixtures in the Yb_2O_3–Fe_2O_3–CoO system, the $YbFeCoO_4$ phase was observed in the powder X-ray pattern but totally disappeared after repeated heating. The $YbFeCoO_4$ phase pre-

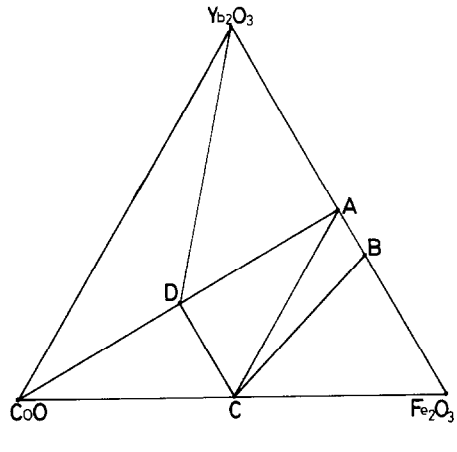

FIG. 2a. The phase diagram of the Yb_2O_3–Fe_2O_3–CoO system at 1350°C in air. (A) $YbFeO_3$, (B) $Yb_3Fe_5O_{12}$, (C) Fe_2CoO_4, and (D) $YbFeCoO_4$.

pared at 1350°C was reheated at 1300°C for 1 week and decomposed to $YbFeO_3$ and CoO. We concluded that $YbFeCoO_4$ was unstable at 1300°C in air. In the previous study (*3*), we reported the phase diagrams of the Ln_2O_3–FeO–Fe_2O_3 systems at high temperatures, and concluded that the $LnFe_2O_4$ phases appeared as stable ones above certain temperatures. We may conclude that each $LnFeMO_4$ compound is stable above some temperature.

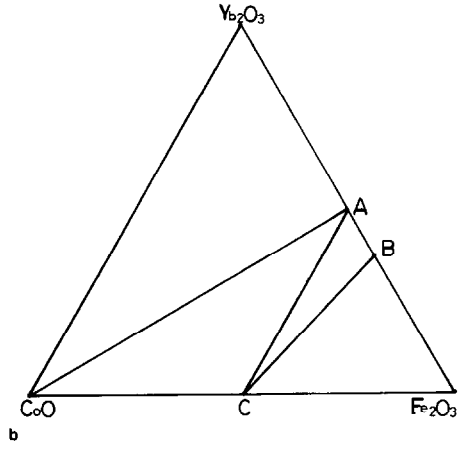

FIG. 2b. The phase diagram of the Yb_2O_3–Fe_2O_3–CoO system at 1300°C in air. (A) $YbFeO_3$, (B) $Yb_3Fe_5O_{12}$, and (C) Fe_2CoO_4.

No solid solution range was detected for any phases at 1300°C. The phase diagram of the Yb_2O_3–Fe_2O_3–CoO system at 1300°C in air is shown in Fig. 2b.

2. The Yb_2O_3–Fe_2O_3–NiO System at 1300 and 1200°C in Air

In the Yb_2O_3–Fe_2O_3 system, there were two phases, $YbFeO_3$ and $Yb_3Fe_5O_{12}$. In the Fe_2O_3–NiO system, there was one stable Fe_2NiO_4 phase. In the NiO–Yb_2O_3 system, there were no ternary stable phases. In the Yb_2O_3–Fe_2O_3–NiO system, there were no quaternary stable phases. As already mentioned (*6*), however we heated the mixture of Yb_2O_3 : Fe_2O_3 : NiO = 1 : 1 : 2 (mole ratio) until the melt phase appeared, no $YbFeNiO_4$ could be obtained. So, the phase relations in the Yb_2O_3–Fe_2O_3–NiO system at 1300 and 1200°C may not change in the temperature region in which a melt phase does not appear. The phase diagram of the Yb_2O_3–Fe_2O_3–NiO system at 1300 and 1200°C in air is shown in Fig. 3. No detectable solid solution range exists for any of the phases.

3. The Yb_2O_3–Fe_2O_3–CuO System at 1000°C in Air

In the Yb_2O_3–Fe_2O_3 system, a single

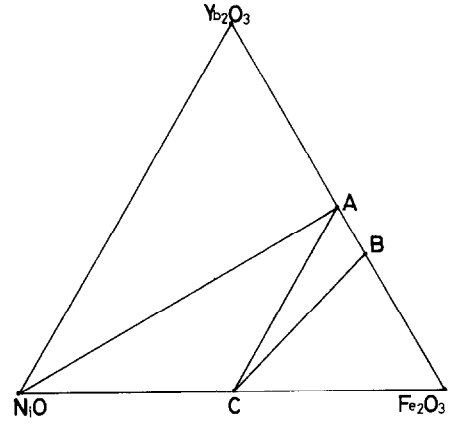

FIG. 3. The phase diagram of the Yb_2O_3–Fe_2O_3–NiO system at 1300 and 1200°C in air. (A) $YbFeO_3$, (B) $Yb_3Fe_5O_{12}$, and (C) Fe_2NiO_4.

phase of $YbFeO_3$ was obtained easily even at 1000°C. In contrast to this, the mixture of $Yb_2O_3 : Fe_2O_3 = 3:5$ (mole ratio), when heated for a month, resulted only in a trace of the $Yb_3Fe_5O_{12}$ phase in the powder X-ray pattern. The $Yb_3Fe_5O_{12}$ prepared at 1300°C was reheated at 1000°C for 1 month. No decomposition to $YbFeO_3$ and Fe_2O_3 was observed. Moreover, when the mixtures of $Yb_2O_3 : Fe_2O_3 : CuO = 15:70:15$, $Yb_2O_3 : Fe_2O_3 : CuO = 15:55:30$, and $Yb_2O_3 : Fe_2O_3 : CuO = 30:55:15$ (mole ratio) were heated for 15 days, the mixtures Fe_2O_3, Fe_2CuO_4, and $Yb_3Fe_5O_{12}$; Fe_2CuO_4 and $Yb_3Fe_5O_{12}$; and $Yb_3Fe_5O_{12}$, Fe_2CuO_4, and $YbFeO_3$ were, respectively, obtained.

TABLE I

POWDER X-RAY DATA FOR $Yb_2Cu_2O_5$

d_{obsd} (Å)	I (%)	d_{obsd} (Å)	I (%)
6.168	4	1.6537	1
4.912	12	1.6388	18
4.046	50	1.6205	1
3.306	1	1.5848	13
3.262	26	1.5803	15
3.159	2	1.5683	10
3.085	9	1.5461	2
2.8901	27	1.5426	5
2.8148	100	1.5349	5
2.6749	80	1.5187	5
2.6345	60	1.5054	19
2.6188	24	1.4826	3
2.5594	3	1.4792	4
2.4270	3	1.4731	7
2.3649	4	1.4443	13
2.2975	3	1.4353	6
2.2421	8	1.4099	5
2.1099	5	1.3628	2
2.0566	12	1.3537	2
1.9997	46	1.3371	2
1.9213	5	1.3324	7
1.8791	34	1.3179	4
1.8158	8	1.3095	4
1.7678	1	1.2735	2
1.7434	23	1.2556	8
1.7160	15	1.2465	9
1.6943	2	1.2235	3
1.6757	7	1.2029	2

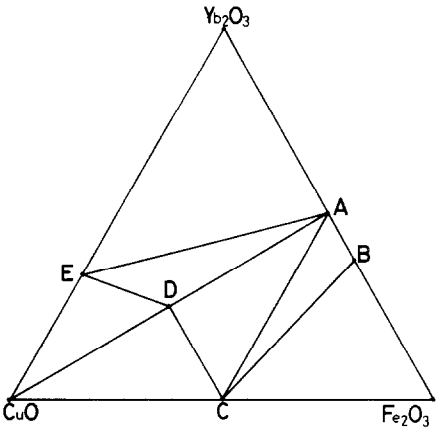

FIG. 4. The phase diagram of the Yb_2O_3–Fe_2O_3–CuO system at 1000°C in air. (A) $YbFeO_3$, (B) $Yb_3Fe_5O_{12}$, (C) Fe_2CuO_4, and (D) $YbFeCuO_4$ and $Yb_2Cu_2O_5$.

It was concluded, therefore, that $Yb_3Fe_5O_{12}$ was stable at 1000°C in air. The Fe_2CuO_4 phase was found in the Fe_2O_3–CuO system, and in the CuO–Yb_2O_3 system there was one new ternary $Yb_2Cu_2O_5$ phase. In order to assure stoichiometry of this new phase, the weight of a mixture of $Yb_2O_3 : CuO = 1:2$ (mole ratio) was checked during the heat treatment, and we concluded that no decomposition of CuO to Cu_2O and oxygen gas occurred in the process and the stoi-

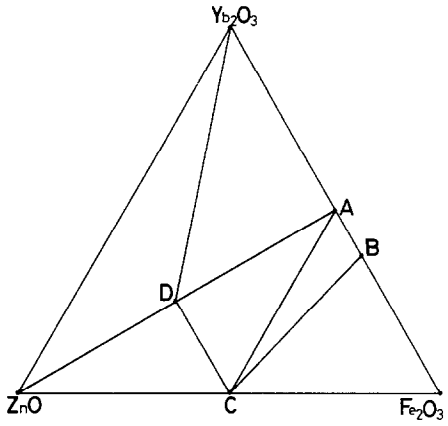

FIG. 5. The phase diagram of the Yb_2O_3–Fe_2O_3–ZnO system at 1300°C in air. (A) $YbFeO_3$, (B) $Yb_3Fe_5O_{12}$, (C) Fe_2ZnO_4, and (D) $YbFeZnO_4$.

TABLE II

THE PHASE RELATIONS IN THE Yb_2O_3–Fe_2O_3–MO SYSTEMS IN AIR AT HIGH TEMPERATURES

System	Composition (mole ratio)	Phase[a]	Time (day)	System	Composition (mole ratio)	Phase[a]	Time (day)
Yb_2O_3–Fe_2O_3–CoO at 1350°C	55 : 25 : 20	1–1–3, Yb_2O_3, 1–1–1–4	7	Yb_2O_3–Fe_2O_3–ZnO at 1300°C	50 : 20 : 30	Yb_2O_3, 1–1–3, 1–1–1–4	5
	30 : 10 : 60	1–1–1–4, CoO, Yb_2O_3	7		20 : 10 : 70	Yb_2O_3, 1–1–1–4, ZnO	5
	10 : 30 : 60	1–1–1–4, 2–1–4, CoO	7		10 : 30 : 60	1–1–1–4, ZnO, 2–1–4	5
	20 : 40 : 35	1–1–1–4, 2–1–4, 1–1–3	7				
	30 : 55 : 15	1–1–3, 3–5–12, 2–1–4	7		25 : 40 : 35	1–1–3, 1–1–1–4, 2–1–4	5
	15 : 70 : 15	3–5–12, 2–1–4, Fe_2O_3	7		25 : 55 : 20	3–5–12, 1–1–3, 2–1–4	5
	25 : 25 : 50	1–1–1–4	7		15 : 70 : 15	3–5–12, 2–1–4, Fe_2O_3	5
					25 : 25 : 50	1–1–1–4	5
Yb_2O_3–Fe_2O_3–CoO at 1300°C	30 : 10 : 60	Yb_2O_3, 1–1–3, CoO	10				
	10 : 30 : 60	1–1–3, 2–1–4, CoO	10	Yb_2O_3–Fe_2O_3–CuO at 1000°C	55 : 25 : 20	Yb_2O_3, 1–1–3, 2–2–5	17
	30 : 55 : 15	1–1–3, 3–5–12, 2–1–4	7		35 : 25 : 40	2–2–5, 1–1–1–4, 1–1–3	17
	15 : 75 : 15	3–5–12, 2–1–4, Fe_2O_3	7		20 : 10 : 70	CuO, 1–1–1–4, 2–2–5	17
					25 : 40 : 35	1–1–1–4, 2–1–4, 1–1–3	17
Yb_2O_3–Fe_2O_3–NiO at 1300 and 1200°C	50 : 20 : 30	Yb_2O_3, 1–1–3, NiO	7		10 : 20 : 70	CuO, 2–1–4, 1–1–1–4	17
	15 : 30 : 55	NiO, 1–1–3, 2–1–4	7		30 : 55 : 15	3–5–12, 1–1–3, 2–1–4	17
		1–1–3, 3–5–12, 2–1–4	10		15 : 70 : 15	3–5–12, Fe_2O_3, 2–1–4	17
	15 : 70 : 15	3–5–12, Fe_2O_3, 2–1–4	10		10 : 0 : 20	2–2–5	15
					25 : 25 : 50	1–1–1–4	15

[a] 1–1–3: $YbFeO_3$; 1–1–1–4: $YbFeMO_4$; 2–1–4: Fe_2MO_4; 3–5–12: $Yb_3Fe_5O_{12}$; 2–2–5: $Yb_2Cu_2O_5$ (M: Co, Ni, Cu, and Zn).

chiometry of the new phase was $Yb_2Cu_2O_5$. The *d*-spacings and relative intensities of the powder X-ray diffraction peaks are listed in Table I. The phase $YbFeCuO_4$ (a = 3.4808(2) Å, c = 24.100(2) Å), which is isomorphous with $YbFe_2O_4$, was found in the Yb_2O_3–Fe_2O_3–CuO system. The phase diagram of the Yb_2O_3–Fe_2O_3–CuO system at 1000°C in air is shown in Fig. 4. No solid solution range in any of the phases was detected.

4. The Yb_2O_3–Fe_2O_3–ZnO System at 1300°C in Air

In the Fe_2O_3–ZnO system, there was an Fe_2ZnO_4 phase, and in the ZnO–Yb_2O_3 system, there was no stable ternary phase. In the Yb_2O_3–Fe_2O_3–ZnO system, the Yb $FeZnO_4$ phase existed as a stable one (a = 3.4251(2) Å, c = 25.282(2) Å). It was isomorphous with $YbFe_2O_4$ (6). The phase diagram of the Yb_2O_3–Fe_2O_3–ZnO system at 1300°C in air is shown in Fig. 5. No detectable solid solution range existed in each stable phase.

The data points which are necessary and sufficient for establishing the above phase diagrams are listed in Table II.

In conclusion, the phase relations in the Yb_2O_3–Fe_2O_3–CoO system at 1350 and 1300°C, the Yb_2O_3–Fe_2O_3–NiO system at 1300 and 1200°C, the Yb_2O_3–Fe_2O_3–CuO system at 1000°C, and the Yb_2O_3–Fe_2O_3–ZnO system at 1300°C were established in air. The $YbFeCoO_4$, $YbFeCuO_4$, and Yb $FeZnO_4$ phases are stable at 1350, 1000, and 1300°C, respectively. They are isomorphous with $YbFe_2O_4$. A new ternary $Yb_2Cu_2O_5$ compound was found in the Yb_2O_3–CuO system at 1000°C in air.

References

1. N. KIMIZUKA AND T. KATSURA, *J. Solid State Chem.* **13,** 176 (1975).
2. N. KIMIZUKA AND T. KATSURA, *J. Solid State Chem.* **15,** 246 (1975).
3. T. KATSURA, T. SEKINE, K. KITAYAMA, T. SUGIHARA, AND N. KIMIZUKA, *J. Solid State Chem.* **23,** 43 (1978).
4. K. KATO, I. KAWADA, N. KIMIZUKA, AND T. KATSURA, *Z. Kristallogr.* **141,** 314 (1975).
5. K. KATO, I. KAWADA, N. KIMIZUKA, I. SHINDO, AND T. KATSURA, *Z. Kristallogr.* **143,** 278 (1976).
6. N. KIMIZUKA AND E. TAKAYAMA, *J. Solid State Chem.* **40,** 109 (1981).
7. N. KIMIZUKA AND E. TAKAYAMA, *J. Solid State Chem.* **41,** 166–173 (1982).
8. B. FISHER AND D. S. TANNHAUSER, *J. Electrochem. Soc.* **111,** 1194 (1964).
9. A. M. M. GADALLA, W. F. FORD, AND J. WHITE, *Trans. Brit. Ceram. Soc.* **62,** 57 (1963).
10. S. J. SCHNEIDER, R. S. ROTH, AND J. L. WARING, *J. Res. Nat. Bur. Stand. Sect. A* **65,** 369 (1961).